NUMERICAL LAYER OPTIMIZATION OF ALUMINUM FIBRE/SAPO-34 COMPOSITES FOR THE APPLICATION IN ADSORPTIVE HEAT EXCHANGERS

G. Füldner[(a,b)], L. Schnabel[(a)], U. Wittstadt[(a)], H.-M. Henning[(a)],
F.P. Schmidt[(b,a)]

[(a)]Fraunhofer Institute Solar Energy Systems,
Heidenhofstr. 2, 79110 Freiburg, Germany
e-mail: gerrit.fueldner@ise.fraunhofer.de
[(b)] Karlsruhe Institute of Technology (KIT),
Kaiserstr. 12, 76131 Karlsruhe, Germany
e-mail: ferdinand.schmidt@kit.edu

ABSTRACT

The design of the adsorptive heat exchanger (AdHex) is a key issue in the development of adsorption heat pumps and chillers. The aim is to increase power densities without decreasing the COP of the machine. One focus has been the development of adsorbent materials with a high water loading at driving temperatures below 100°C. SAPO-34 has proved to be a very promising material for these applications (Henninger et al., 2010).

As a consequence, the design of the AdHex has to be adapted to the needs as well: more heat must be removed and supplied more quickly from and into the active material, while for high COP a good mass ratio between adsorbent and heat exchanger has to be realized. For this purpose a new composite material has been developed. It consists of aluminum fibres (Andersen et al., 2008) realizing a high volumetric surface at high porosities, good thermal conductivity and good thermal contact to a metal lamella (Wittstadt et al., 2009). These fibres then are coated with SAPO-34 by direct crystallization (Bauer et al., 2009). Results of adsorption kinetics measurements and simulations on lab scale samples of such composites show a fast uptake at a very good mass ratio. Heat and mass transport coefficients of the samples are obtained by fitting a bidisperse non-isothermal model to the transient adsorption kinetics in large pressure jump (LPJ) experiments. Additionally, heat conductivity, heat capacity, density, pore size and porosity are determined. With the obtained physical parameters cycle simulations are performed and the geometric dimensions of the composite layer are optimized with respect to a high volume specific power (> 250 W per liter of AdHex volume) at good cooling COP values (>0.5 without heat recovery) at moderate cycle conditions (15°C/40°C/95°C).

1. EXPERIMENTAL SAMPLE CHARACTERISATION

To obtain heat and mass transfer parameters samples have to be prepared which vary in geometry but if possible not in material properties. On a macroscopic level it is often not easy to produce adsorbent (composite) samples with e.g. different layer thicknesses but otherwise similar properties. Besides, the homogeneity of properties throughout the sample thickness is not always given. This has to be kept in mind when using such samples to validate numerical models.

1.1. Sample preparation and determination of physical parameters

For this study, four samples have been prepared and characterised in detail. Two samples consist of a sintered aluminum fibre layer of 2 mm and 4 mm thickness, sintered to a thin aluminum sheet (Andersen et al., 2008). Figure 1 shows pictures of the 2 mm sample IFAM 1378. This structure has a very high porosity (approx. 70%, see Table 1) and thus a very high volume specific surface. In a second step a compact SAPO-34 layer has been synthesized in situ onto the fibre support by a Partial Support Transformation (PST) method by SorTech AG (Bauer et al., 2009).
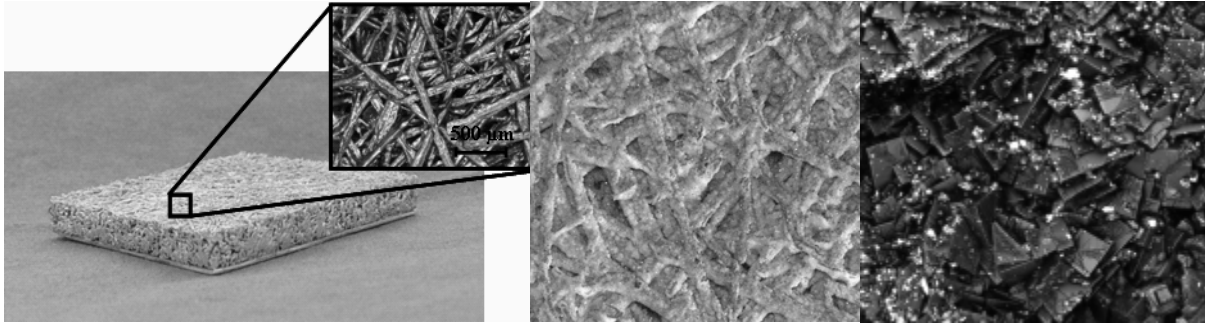

Figure 1 – Sample IFAM 1378: Fibres sintered to an aluminum sheet without adsorbent (left, full sample size 30x30mm^2), fibres with SAPO-34 deposition (middle, fibre thickness ~120μm), laser scanning microscope picture of SAPO-34 crystals on fibre (right, crystal size ~10-20μm).

Two reference samples consist of 2 mm aluminum sheets on which again SAPO-34 has been synthesized in two layer thicknesses. The samples have been characterized extensively with different methods to obtain the physical parameters necessary for a physical model of the adsorption kinetics. The porosity of the pure aluminum fibre carrier structures can easily be determined knowing the bulk aluminum density (AlCu5, 3 g/cm^3). To determine the mean structural pore size of the uncoated and the coated material by permeability measurements, additional samples without aluminum sheet sintered to the bottom have been prepared. These measurements as well as fibre characteristics and the visual impression of the images obtained with a laser scanning microscope give an equivalent pore size of the uncoated fibres of around 350-400 μm. For coated samples the structural pores show an equivalent diameter in the range of 200-250 μm. This is also consistent with micro-CT scans of the coated composite which show a distribution of adsorbent layer thicknesses with one peak at about 10 μm and a second at about 70 μm. Table 1 gives detailed information on the sample properties.

Table 1 – Sample properties.

	Composite thickness [mm]	Adsorbent mass [g]	Fibre mass [g]	Ψ fibres [%]	ρ_{kris} [kg/m^3]	$\rho_{ads,comp}$ [kg/m^3]	ρ_{comp} [kg/m^3]	λ [W/(m K)]
IFAM 1378	2.11	1.1	1.43	75	1500	580	1330	8
IFAM 1387	3.94	2.2	3.37	68	1500	620	1570	8
Sortech 2	0.04	0.15	-	-	1500	1500	-	0.5
Sortech 3	0.027	0.093	-	-	1500	1500	-	0.5

Thermal conductivity of both the pure fibres (λ=14 W/(m K)) and the composite have been measured with a Netzsch LFA 447 Nanoflash®.

1.3. Measurement of transient adsorption process
The kinetics measurement facility consists of two vacuum chambers that can be connected by valves. They are located in a large box which is kept at constant temperature.
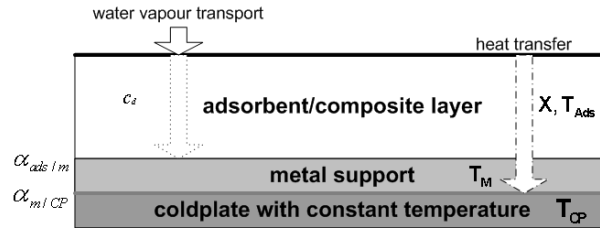

Figure 2 – Schematical presentation of a sample on the coldplate, heat transfer is influenced by the thermal conductivities of the adsorbent (composite) layer and the metal support as well as the two heat transfer coefficients between the layers.

The small measuring cell contains the sample fixed onto a plate that can be passed through by water at constant temperature ("coldplate"). The pressure and temperature within the water vapour reservoir and the measuring cell are recorded. Additionally, with a heat flux sensor it is possible to measure the heat flux between the sample and the coldplate. More details such as the characteristics and accuracy of the sensors can be found elsewhere (Schnabel et al., 2010; Schnabel and Füldner, 2009). As a consequence of too long response times of the formerly installed thin film Ni-100 temperature sensor, the surface temperature measurement has been adapted and is now carried out using an infrared thermometer (Optris CT LT) located above the sample. Although the stationary accuracy is by now only +/- 1 K, the dynamic accuracy by far outperforms the behaviour of a resistance temperature sensor; a temperature rise will be detected quasi instantaneously which is crucial when performing large pressure jump (LPJ) experiments. In the measurements the activation (desorption) conditions, the adsorption conditions (starting pressure and temperature) and the sample setup (coupling to the coldplate) can be varied. For example the use of heat conductive paste (thermigrease, TG) when coupling the sample to the coldplate leads to a faster adsorption process since the heat transfer coefficient $\alpha_{m/CP}$ is higher.

2. PARAMETER IDENTIFICATION WITH NUMERICAL MODELS
For a geometric optimization of the AdHex unit it is mandatory to use a mathematical-physical model which describes the actual physics of the coupled heat and mass transport processes on the adequate scale. To this end measurements of the transient adsorption process have been modelled in the commercial FEM software COMSOL Multiphysics 3.5. By finding sets of parameters which describe both pressure signal and surface temperature (and additionally the heat flux signal if measured), and in which only the parameter which has been changed in the measurement (coupling to coldplate, starting pressure, desorption condition) has to be adapted to describe different measurements, the model can be validated and transport coefficients identified.

2.1. Monodisperse and bidisperse models of non-isothermal adsorption kinetics
First, a one-dimensional monodisperse non-isothermal model has been implemented. This model is described in detail elsewhere (Füldner and Schnabel, 2008). It includes the energy balance with heat transfer inside the composite layer (heat conductivity λ, loading dependent heat capacity $c_{p,ads}$, mean composite density ρ), heat transfer within the metal carrier sheet and the two heat transfer coefficients composite/metal $\alpha_{ads/m}$ and

metal/coldplate $\alpha_{m/CP}$. The mass balance is a single diffusion equation with a sink and an effective diffusion coefficient. With this model, the transient adsorption process in a homogenous adsorbent layer can be described very well. It has to be noted, though, that the diffusion coefficients found with this kind of modelling might not be physical parameters that scale adequately with different layer thicknesses. For composite materials such as pellets and much more for the considered fibre composites, they have to be regarded as effective mass transport parameters, being valid only for the layer thickness for which they have been fitted to a measurement. If it is not possible to describe various composite thicknesses with one single diffusion coefficient (i.e. when the macropore transport is not the only limiting factor), a bidisperse non-isothermal model of the composite has to be used. In literature, bidisperse models have been used either for packed beds of pellets or for bidisperse pellets which are assumed to consist of spherical adsorbent particles with a connecting network of macropores around (e.g. Sun and Meunier, 1987 a+b).

Our model assumes a different geometry: cylindrical structural pores are surrounded by a hollow cylinder of adsorbent. Transport in the structural pores is calculated as a superposition of viscous flow and Knudsen diffusion, depending on the pore size (Kast and Hohenthanner, 2000). Transport in the adsorbent layer is modelled as a concentration driven diffusion with a Darken factor (Reyes et al., 2000).

The adsorbent layer thickness of the hollow cylinder geometry

$$d_{kris} = \frac{d_{pore}}{2} \sqrt{\frac{\left(1 - V_{fib}\big/V_{comp}\right)}{\Psi_{MP}} - 1} \qquad \qquad 1)$$

is directly linked to the pore diameter of the structural pores of the composite d_{pore} and composite macro-porosity

$$\Psi_{MP} = 1 - \frac{V_{kris} + V_{fib}}{V_{comp}}. \qquad \qquad 2)$$

V_{kris} and V_{fib} specify the volume of the adsorbent layer and the volume of the fibres in the composite. For a pore diameter of 250μm this gives a mean layer thickness of about 50μm, which is in good agreement with the sample characterization described in Section 1.1.

The transport equation in the structural pores takes on the form

$$\frac{\partial c_{MP}(z,t)}{\partial t} = \frac{\partial}{\partial z} D_{Kast} \frac{\partial c_{MP}(z,t)}{\partial z} - \frac{4 * \Phi(z,t) * \Psi_{kris}}{d_{pore}}. \qquad \qquad 3)$$

The porosity Ψ_{kris} of the adsorbent layers has been calculated from density (about 1.5 g/cm^3) and pore volume from nitrogen adsorption (about 0.27 cm^3/g), see Table 2. Mass transport in the adsorbent layer is calculated by a second diffusion equation

$$\frac{\partial c_{kris}(z,r,t)}{\partial t} = \frac{\partial}{\partial r} D_{kris} \frac{d \ln p}{d \ln X} \frac{\partial c_{kris}(z,r,t)}{\partial r} - \frac{1}{M} \frac{\rho_{kris}^{dry}}{\Psi_{kris}} \frac{\partial X(z,r,t)}{\partial t}. \qquad \qquad 4)$$

Within the adsorbent layer instantaneous adsorption as a function of pressure p(z,r,t) and temperature T(z,t) is included as a sink of the mass balance. The two processes are coupled by the normal diffusive flux

$$\Phi(z,t) = -D_{kris} \left. \frac{\partial c_{kris}(z,r,t)}{\partial r} \right|_{r=R_{MP}} \qquad 5)$$

into the adsorbent layer at the surface of the macropores (r=R_{MP}) for each height z. Heat transfer is modelled only in the z-direction perpendicular to the composite surface; this implies the assumption that heat transport from the adsorbent surface to the metallic carrier structure is very fast, which is reasonable considering the very thin layers and very good contact between adsorbent and fibre.

2.2. Parameter identification
Adsorption kinetics of the two single layer samples (Sortech 2+3) have been simulated with the monodisperse model. The two single layer samples can be fitted very well with the monodisperse model, experimental results (grey symbols) for pressure drops and surface temperatures from some exemplary measurements (desorption against vacuum pump at 95°C, two different starting pressures) are shown in Figure 3 together with the simulated results (black symbols).
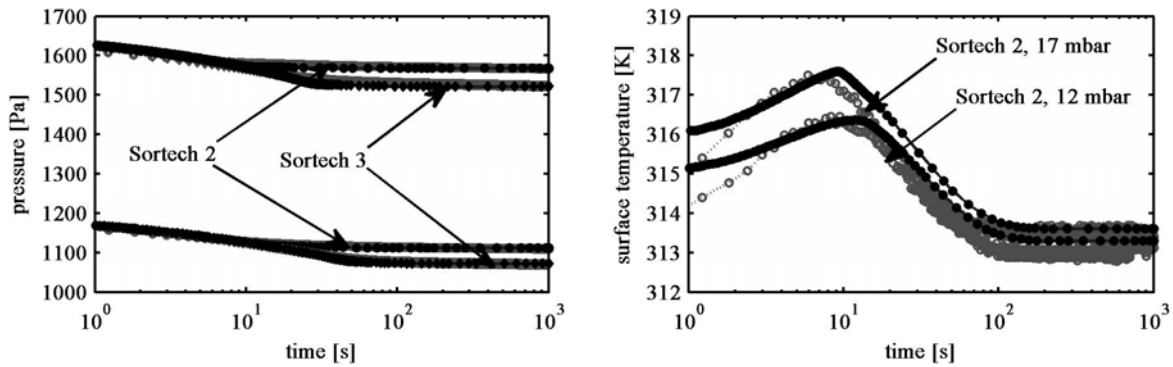

Figure 3 – Adsorption kinetics of the two pure adsorbent layer samples: measured pressure signals(grey) for both samples, two different starting pressures (left), for a better overview only surface temperatures of Sortech 2 for the two starting pressures (right). Simulated results for single layer samples Sortech 2 (o) and Sortech 3 (◊) in black. Parameters for the simulation can be found in Tables 1 and 2.

Samples IFAM 1378 and IFAM 1387 with comparable densities, porosities, adsorbent layer thicknesses and structure pore sizes can be fitted as well using the monodisperse model. Simulation parameters from best fits are given in Table 2. Two different diffusion coefficients D_{eff}=1.3*10^{-3} m^2/s (1378) and D_{eff}=3.7*10^{-3} m^2/s (1387) are found for the two different thicknesses. An optimization of the fibre layer thickness is not meaningful with the monodisperse model since the effective diffusion coefficient D_{eff} is a function of the layer thickness. With the assumption of a bidisperse model, with the adsorbent layer diffusion coefficient D_{kris}=4*10^{-6} m^2/s found in the monodisperse simulation of the thin adsorbent layers and similar heat transfer parameters as used in the monodisperse modelling of the composite samples, it is possible to describe both composite samples with one set of parameters.

Table 2 – Transport parameters used in simulation.

	$\alpha_{m/CP}$ [1] [W/(m² K)]	$\alpha_{ads/m}$ [W/(m² K)]	$c_{p,eff}$ [J/(kg K)]	Ψ / Ψ_{kris} [%]	d_{pore} [m]	D_{eff} [m²/s]
IFAM 1378	130/1200	5000	900	40/40	2.5×10^{-4}	1.3×10^{-3}
IFAM 1387	180/1500	5000	900	26/40	2.5×10^{-4}	3.7×10^{-3}
Sortech 2	180/1500	5000	900	- /40	-	$2\text{-}4 \times 10^{-6}$
Sortech 3	180/1500	5000	900	- /40	-	$2\text{-}4 \times 10^{-6}$

The fits of simulations (black symbols) with the bidisperse model to various experimental results (grey symbols) can be seen in Figure 4.
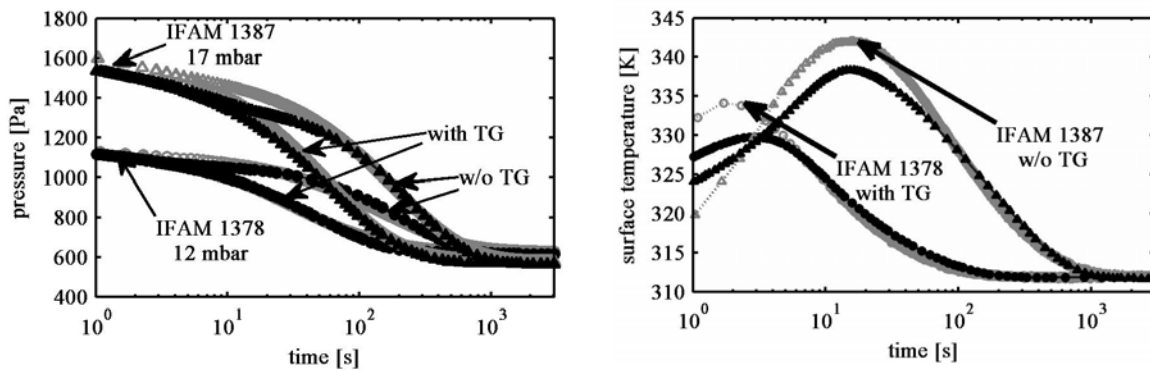

Figure 4 - Adsorption kinetics: pressure signal in measurement chamber (left), surface temperature of samples (right) and simulated results (black) for samples IFAM 1378 (o) and IFAM 1387 (Δ). Experimental results (grey) show LPJ measurements with desorption against vacuum pump at 95°C, sample coupling to the coldplate with and without thermigrease (TG). Parameters for the simulation can be found in Table 1 and 2.For a better overview, only two of the four surface temperature measurements and simulations are depicted.

The largest deviations are found for the first 10-30 s. One reason for this is the description of adsorption equilibria, a generalized characteristic curve, which differs slightly from the SAPO-34 behaviour in some regions of the adsorption potential. Of course, some deviations can also be attributed to the inhomogeneity of the samples, e.g. a distribution of adsorbent layer thicknesses and pore sizes.

3. SIMULATION OF CYCLES AND GEOMETRY OPTIMIZATION
With a well defined set of parameters it is now possible to predict the behaviour of composite layer thicknesses which have not been characterised experimentally.

3.1. Assumptions on AdHex geometry and cycle conditions for optimization
With the fibre/SAPO-34 composite described above, a new flat plate adsorbent heat exchanger (AdHex) can be designed. Figure 5 shows a picture and a scheme of the proposed geometry (Wittstadt et al., 2009). It has been shown that this setup can have advantages over the standard finned tube setup. A prototype has been built and presented (Füldner et al., 2010).

---

[1] For the heat transfer coefficient between metal sheet and coldplate $\alpha_{m/CP}$ two values are given – one refers to the sample coupled to the coldplate without, the other with thermigrease.

The fluid channels are made from extruded aluminum profiles supplied by Erbslöh AG. The fibre sheets have been brazed onto the profiles by Fraunhofer IFAM. Thereafter, the adsorbent layer has been directly crystallised onto the structure by SorTech AG. A complete adsorptive heat exchanger would be made from a stack of the depicted element. The distributor and collector pipe are not optimised yet, an adapted design will lead to a reduction in both dead volume and thermal mass. To demonstrate a way of optimizing the fibre layer thickness, assumptions on the geometry of the AdHex have been chosen according to this prototype.

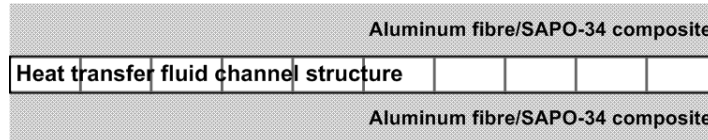Cross section through aluminum profile with composite:

Figure 5 –AdHex prototype and scheme of geometry with square fluid channels and fibre composite.

The cycle conditions under which this optimization has been carried out are typical conditions encountered e.g. in car air conditioning with a desorption temperature of 95°C, evaporator temperature of 15°C and cooling loop temperature of 40°C. The modelling implies the somehow idealized assumption of isobaric conditions in evaporator/condenser and instantaneous switching from heating to cooling loop temperature. Transport parameters have been chosen according to the results of the parameter identification from the kinetics measurement. The heat transfer coefficient between fluid channel surface and heat transfer fluid has been set to 1000 W/(m² K) which is a reasonable number for the depicted geometry. For cycle control, a fixed half-cycle time has been chosen to switch between ad- and desorption. Then, both cycle time and fibre layer thickness have been varied. Two key figures have been calculated: The thermal coefficient of performance (COP) for cooling (basic one adsorber cycle without heat recovery) and the volume specific cooling power (VSCP). As one possible optimization criterion, the product of cooling COP and VSCP has been chosen.

3.2. Optimization of composite layer thickness
A vast amount of parameter variations have been carried out both with the monodisperse and the bidisperse model to explore to which extent the results differ. Figure 6 shows a mesh plot of the product of COP and VSCP over a range of cycle durations and fibre layer thicknesses, simulated in the bidisperse model with parameters given in Table 2. The maximum is found at a thickness of about 2 mm and optimum cycle duration of 150 s. When calculated with the monodisperse model and a diffusion coefficient $D_{eff}=1.3*10^{-3}$ m²/s from sample IFAM 1378, the maximum would lay at cycle durations around 100 s and a composite layer thickness of about 1.5 mm, with the higher diffusion coefficient from sample IFAM 1387 at even lower values.
The maximum volume specific cooling power (VSCP) that is reached with the parameters measured for the two samples in the bidisperse model is about 250 W/L of AdHex volume over the full cycle, see Figure 7.
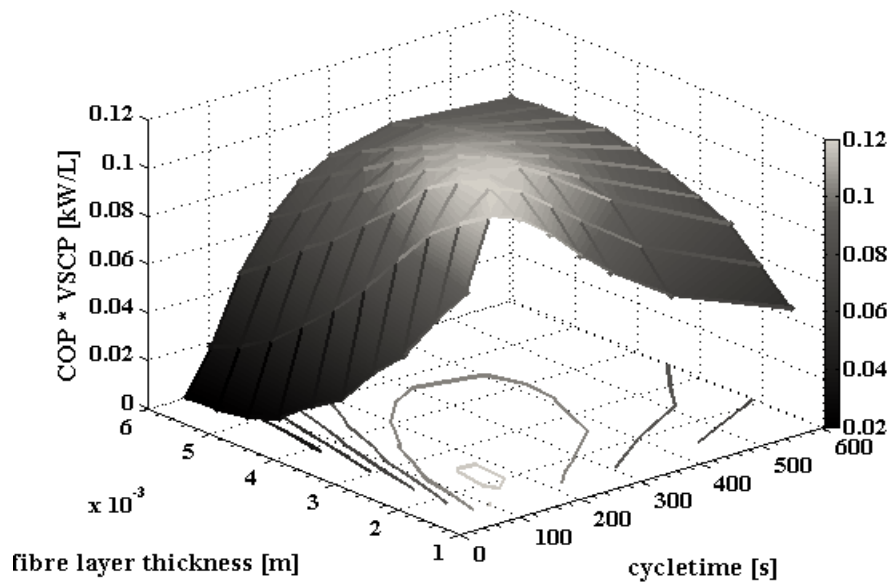
Figure 6 - Product of COP and VSCP over fibre layer thickness and cycle durations: Results from parameter variation with bidisperse model, for parameters see Table 2.
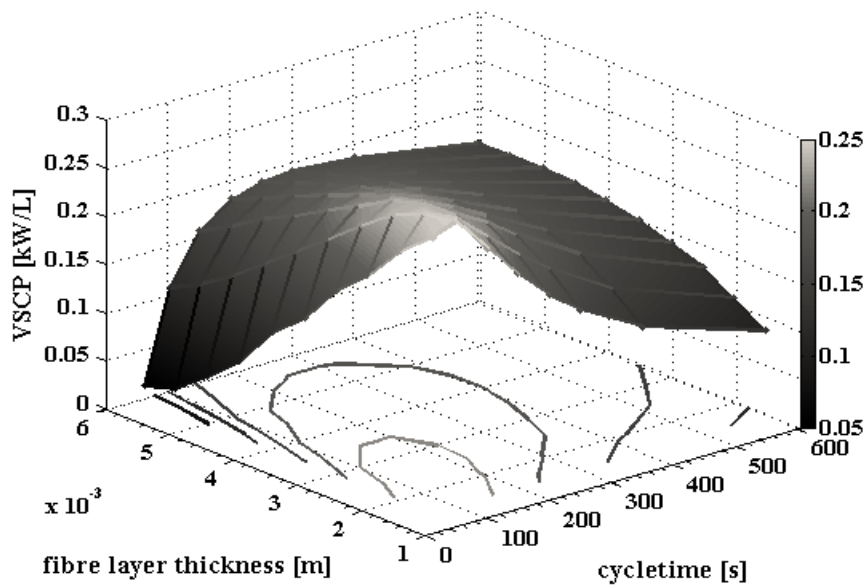

Figure 7 - VSCP over fibre layer thickness and cycle durations: Results from parameter variation with bidisperse model, for parameters see Table 2.

The maximum in cooling COP without any heat recovery mechanism is found to be slightly above 0.5. A map of COP values depending on cycle time and fibre layer thickness is shown in Figure 8. In the limit of short cycle times, the COP increases with decreasing thickness of the fibre layer, since the cycle time is too short to achieve a high loading spread between ad- and desorption in the composite layer.
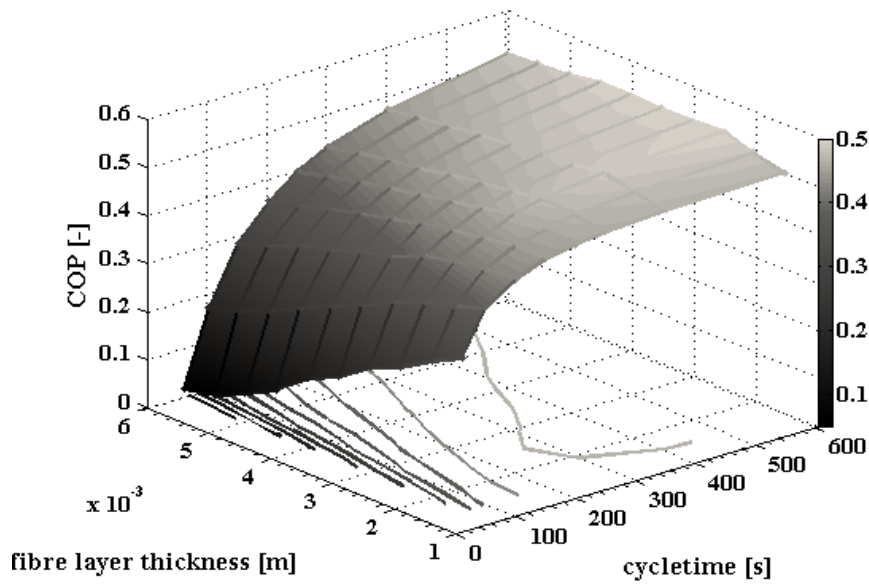
Figure 8 - COP over fibre layer thickness and cycle durations: Results from parameter variation with bidisperse model, for parameters see Table 2.

In the opposite limit of long cycle times, the highest values can be reached for the thickest composite layer since even the thickest layer can achieve its full loading spread, and the dead thermal masses of fluid channels (which stay the same irrespective of the layer thickness) fall into account less.

4. CONCLUSION

A detailed non-isothermal bidisperse model of heat and mass transfer during adsorption of water in an aluminum fibre/SAPO-34 composite has been set up in COMSOL Multiphysics. To find physically meaningful transport parameters, the model has been calibrated and validated with measurements on 4 samples: Two pure adsorbent layers of different thickness and two composite samples of different thickness. It could be shown that under certain boundary assumptions, this model can be applied to predict an optimal composite layer thickness e.g. with respect to the product of COP and VSCP.

Both experimental and simulation results show that by the use of an aluminum fibre/SAPO-34 composite in a flat plate geometry fast adsorption cycles at good adsorbent/metal mass ratios are technically feasible. For such composites the main limitation is on the fluid side: Switching from ad- to desorption temperature and thermal contact between fluid and heat exchanger have to be enhanced from state-of-the-art to realize fast cycles in adsorption heat pumps.

NOMENCLATURE

α	heat transfer coefficient, $W/(m^2 \, K)$	V	volume, m^3
λ	heat conductivity, $W/(m \, K)$	X	water loading, kg_{H2O}/kg_{ads}
ρ	density, kg/m^3	*Other super-/subscripts:*	
Φ	vapor flux, $mol/(m^2 \, s)$	*ads*	of the adsorbent
Ψ	porosity	*comp*	of the composite
c	vapor concentration, mol/m^3	*CP*	of the coldplate
c_p	specific heat capacity, $J/(kg \, K)$	*dry*	of the dry adsorbent
d_{kris}	adsorbent layer thickness, m	*eff*	effective
d_{pore}	structural pore diameter, m	*fib*	of the fibres
D	diffusion coefficient, m^2/s	*kris*	of the adsorbent layer
p	pressure, Pa	*m*	of the metal sheet
T	temperature, K	*MP*	of the macropores

REFERENCES

1. Andersen O., Studnitzky T., Kostmann C., and Stephani G., 2008, Sintered Metal Fibre Structures from Aluminum Based Fibres - Manufacturing and Properties, *Proc. of Cellmet 2008*, Fraunhofer IFAM Dresden, Germany:24-29.

2. Bauer J., Herrmann R., Mittelbach W., and Schwieger W., 2009, Zeolite/Aluminum Composite Adsorbents for Application in Adsorption Refrigeration, *Int. J. Energy Research* 33(13):1233 − 1249.

3. Freni A., Bonaccorsi L., Proverbio E., Maggio G., and Restuccia G., 2009, Zeolite Synthesised on Copper Foam for Adsorption Chillers: A Mathematical Model, *Miropor. Mesopor. Mat.* 120(3):402 − 409.

4. Füldner G. and Schnabel L., 2008, Non-isothermal kinetics of water adsorption in compact adsorbent layers on a metal support, *Proc. of the Int. COMSOL Conf.*, Hannover, Germany.

5. Füldner G., Wittstadt U., Schnabel L., Schmidt F.P., Schossig P., and Henning H.M., 2010, Design and Analysis of a Highly Efficient Adsorbent Heat Exchanger, *Proc. of the 1. Int. Conf. on Materials for Energy*, Karlsruhe, Germany: B/1045 − 1047.

6. Henninger S.K., Schmidt F.P. and Henning H.-M., 2010, Water Adsorption Characteristics of Novel Materials for Heat Transformation, *J. Appl. Therm. Eng.* 30(13):1692-1702.

7. Kast, W. and Hohenthanner, C., 2000, Mass Transfer within the Gas-Phase of Porous Media, *International Journal of Heat and Mass Transfer* 43:807-823.

8. Reyes, S. C., Sinfelt, J. H., and DeMartin, G. J., 2000, Diffusion in Porous Solids: The Parallel Contribution of Gas and Surface Diffusion Processes in Pores Extending from the Mesoporous Region into the Microporous Region, *J. Phys. Chem. B, ACS* 104:5750-5761.

9. Schnabel, L., Tatlier, M., Schmidt, F., and Erdem-Senatalar, A.,2010, Adsorption Kinetics of Zeolite Coatings Directly Crystallized on Metal Supports for Heat Pump Applications, *J. Appl. Therm. Eng.* 30(11-12):1409 − 1416

10. Schnabel L., Füldner G. 2009, Water Adsorption in Compact Adsorbent Layers – Kinetic Measurements and Numerical Layer Optimization, *Proc. of Heat Powered Cycles 2009*, TU Berlin, Germany: 520.

11. Sun, L. and Meunier, F., 1987a, A Detailed Model for Nonisothermal Sorption in Porous Adsorbents, *Chem. Eng. Sci.* 42:1585 − 1593.

12. Sun, L. and Meunier, F., 1987b, Non-isothermal Adsorption in a Bidisperse Adsorbent Pellet, *Chem. Eng. Sci.* 42:2899 − 2907.

13. Wittstadt U., Füldner G., Schnabel L., and Schmidt F.P. 2009, Comparison of the Heat Transfer Characteristic of Two Adsorption Heat Exchanger Concepts, *Proc. of Heat Powered Cycles 2009*, TU Berlin, Germany: 470.